J. Appl. Comput. Mech., 5(2) (2019) 381-389
DOI: 10.22055/JACM.2018.25941.1301

ISSN: 2383-4536
jacm.scu.ac.ir

M&MoCS

Shahid Chamran University of Ahvaz

Journal of Applied and Computational Mechanics

Research Paper

On the Use of Acoustic Emission and Digital Image Correlation for Welded Joints Damage Characterization

Kadhum Shrama[1], Safaa Kh Al-Jumaili[2], Rhys Pullin[3], Alastair Clarke[4], Sam L. Evans[5]

[1] Iraqi Ministry of Electricity, General Directorate of Electrical Energy production
Basrah, Basrah, Iraq, drkadhumshrama@gmail.com
[2] Department of Materials Engineering, University of Basrah
Basrah, Iraq, SafaaKh@gmail.com
[3] School of Engineering, Cardiff University
The Parade, CF24 3AA, Cardiff, UK, PullinR@cf.ac.uk
[4] School of Engineering, Cardiff University
The Parade, CF24 3AA, Cardiff, UK, ClarkeA7@cf.ac.uk
[5] School of Engineering, Cardiff University
The Parade, CF24 3AA, Cardiff, UK, EvansSL6@cf.ac.uk

Received May 21 2018; Revised October 05 2018; Accepted for publication October 07 2018.
Corresponding author: Kadhum Shrama, drkadhumshrama@gmail.com

Abstract. A series of tests have been conducted to investigate fatigue damage characterization in corroded welded steel plates using structural health monitoring (SHM) techniques. Acoustic Emission (AE) is a non-destructive testing (NDT) technique with potential applications for locating and monitoring fatigue cracks in service. In the present work, AE is implemented to characterize damage during crack evolution. It is considered to be based on the relationship between RA value (the rise time divided by the amplitude) and the average frequency of the recorded data. Results are confirmed by visual observation of the crack geometry at the end of the test and by Digital image correlation (DIC) measurements. It is seen that the obtained results allow a better understanding of such damage mechanisms, and enabling an early warning against final failure. Thus, ensuring the safety and integrity of the structures is feasible.

Keywords: Fatigue, Welded steel, Damage characterization, Acoustic Emission, Digital Image Correlation.

1. Introduction

Fatigue phenomena associated with the welded steel components is one of the major issues that negatively affects the integrity of a structure. In real industrial applications, welded components face deterioration due to several problems. For example, automotive chassis failure has potentially catastrophic consequences. Their structural durability is reduced by factors including the ageing of protective coatings, stone chipping, and environmental effects like corrosion resulted from salty roads in winter as well as welding effects [1]. Therefore, assessment of damage and deterioration in safety-critical structures is in great demand and is vital to maintain the structure both for safety and economic considerations.

The acoustic emission technique offers great potential for using as a structural health monitoring (SHM) tool. The technique uses piezoelectric transducers to detect elastic stress waves which are released by the growth of damage [2]. By analysis of the resultant waveform in terms of feature data such as amplitude, energy and time of arrival, the severity and location of the AE source can be assessed [3]. One of the techniques to classify damage is based on the recorded waveform shape. The waveform shape depends on the cracking mode and can be used for the classification of cracks in different

Published online: March 21 2019

materials [4, 5]. For example, the shape of the initial part of the waveform can be defined by the RA value [6]. RA value is the rise time (RT) divided by the amplitude (A) measured in (μs/v or ms/v). The rise time of the signal can be defined as the interval between the first threshold crossing and the maximum amplitude of the signal. Furthermore, the vertical axis is the amplitude of a signal in volts and the horizontal scale is the elapsed time from the point of triggering. The amplitude in dB of an AE signal is calculated relative to a 1μV reference voltage at the transducer. To do so, an AE acquisition system by using the equation (amplitude (dB) = 20 log (Vs/Vref)) is used. Figure 1 indicates how the RA value can be implemented to characterize the fracture mode. Figure 2 displays more advanced characterization analysis by means of the relationship between RA and average frequency (the ratio of threshold crossings (counts) divided by the duration of the signal and measured in kHz) to define the type of cracking, as reported in [7-10]. Where AE signal has low average frequency and high RA value, it was classified as originating from a shear-type crack/movement. However, signals with high average frequencies and low RA values were classified as originating at tensile cracks.

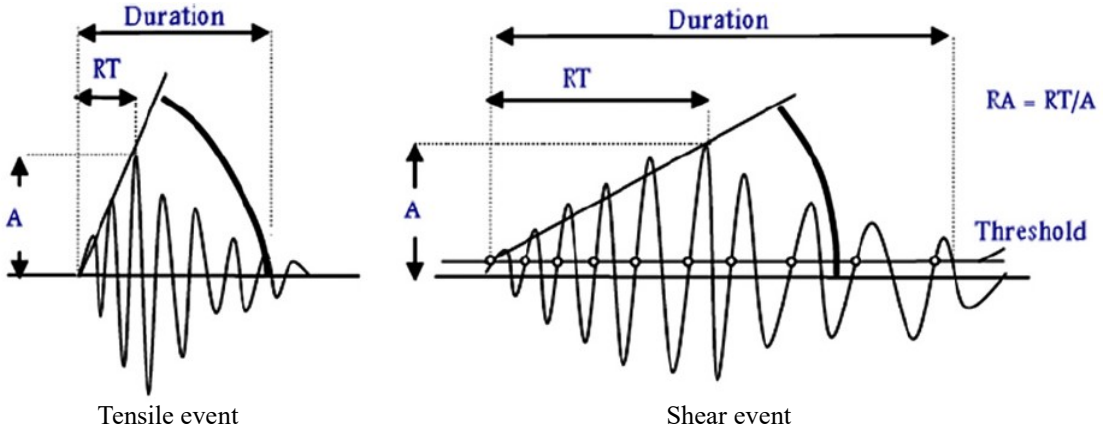

Fig. 1. Cracking modes and corresponding AE signals [9].

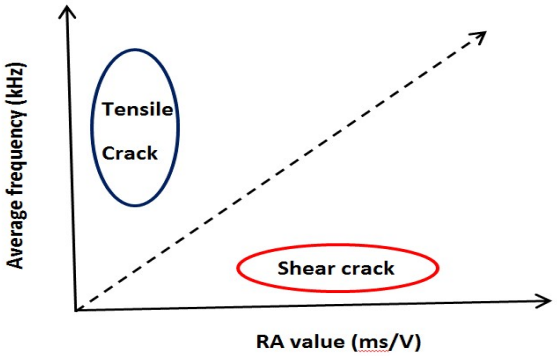

Fig. 2. Classification of cracking.

Using this technique, several researchers have conducted investigations on different materials such as concrete, composites, and metals. For example, cracking mode classification in cementitious material under four-point bending tests has been studied by Aggelis [11]. It is reported that this classification enables a warning against final failure. Elfergani et al. [9] investigated damage assessment due to corrosion in pre-stressed concrete and found that tensile and shear movements can be distinguished. Shahidan et al. [8] performed laboratory experiments on a reinforced concrete beam tested by four-point bending and stated that the technique can indicate the type and level of damage. Thus, the safety conditions and integrity of the reinforced concrete beam due to the loading process will be known. Ohno and Ohtsu [7] have studied the crack classification in reinforced concrete under four-point bending tests. The outcomes showed good agreement with simplified Green's functions for moment tensor analysis (SiGMA). The same approach was adopted to classify damage in composites. The waveform shape was used to classify delamination and matrix cracking signals in large scale carbon fiber plates under buckling [12-14] and fatigue loading [15].

Other researchers investigated metallic fatigue damage characterization using this approach. Aluminum plates have been tested by Aggelis et al. [16] and the results exhibited that the RA value increased sharply (approximately 1000–1200 cycles before final failure) which can be used as an alarm before the final failure. Also, the monitoring of metallic materials under monotonic and fatigue loading has been carried out by Kordatos et al. [10] for measuring damage propagation and dominant fracture modes. They found that the shift of both average frequency and RA value is attributed to the shift of dominant fracture modes.

Experimental fatigue tests typically require large testing times. This time will considerably increase when one period has to interrupt the fatigue test to manually measure crack lengths or specimen extension. To avoid this limitation, in this study, the Digital Image Correlation technique is applied to determine the initiation of cracking to compare with the detected AE. Previous studies have been conducted utilizing the combination of DIC and AE under fatigue loading. For example, Pullin et al.

[18, 19] used the combination of two techniques under fatigue loading. The former was carried out on four-point bending fatigue of aerospace steel and the latter was performed on the detection of cracking in gear teeth under fatigue loading. The authors pointed out that the method of crack monitoring had to be non-contact, so not to produce frictional sources of AE in the crack region. Kovac et al. [20] implemented both techniques to monitor AISI 304 stainless steel specimens subjected to constant load and exposed to an aqueous sodium Thiosulphate solution. Aggelis et al. [17] also utilized both methods to monitor the bending failure of concrete beams reinforced by external layers of different composite materials.

This study highlights using of two techniques as they have complementary advantages and disadvantages. In addition, the RA value method has been extensively utilized in the AE technique for numerous applications in concrete. On the other hand, there has been little research on metal to obtain the relationship between tensile and shear movement or into the damage classification of metal plates. This paper investigates the use of AE and DIC techniques to classify the nature of damage occurring in welded steel specimens under a fatigue loading regime. The relationship between RA and average frequency is used as an identification tool between tensile and shear cracks. Results' validation is achieved by comparison with the strain field measured using DIC techniques.

2. Experimental Procedure

2.1 Specimen preparation

Each specimen test is made from two plates of dimensions (120 cm×140 mm×2.78 mm) which are welded along the 120 cm line. The welded rectangular "blank" product is then cut to manufacture the final design of the fatigue specimens (Fig. 3). This manufacturing process ensures that there is a continuous weld with no start/stop weld locations which may affect the fatigue behavior.

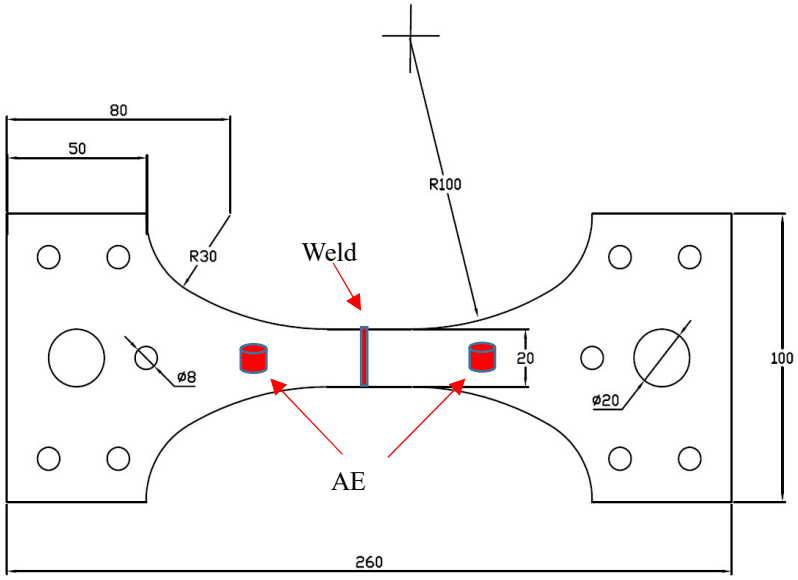

Fig. 3. Details of fatigue specimen geometry (dimensions are in mm).

The fatigue dog-bone specimens are manufactured from FB590 which is a high-strength steel plate (0.2% proof stress 550 MPa, ultimate strength 600 MPa, and elongation 12% based on three coupon tests). Part of the specimens is subjected to alternating spraying of 5% Na-Cl solution according to the corrosion procedure as explained in SAEJ2332 [21]. The specimens are experiencing a fatigue load ranging from 41% to 85% of the ultimate tensile strength with a stress (R) ratio of 0.1 and a frequency of 5Hz. The fatigue specimens are held on pinned joints in a Losenhausen servo-hydraulic testing machine (maximum force 100kN) with an MTS Flex Test controller.

Before testing, the specimens are typically coated to provide the first line of defense against corrosion, with Electro coating (e- coating) acting as a primer layer for subsequent paint, which is beneficial for simulating real-life metal applications. E-coating is carried out in TATA Steel IJmuiden, where all of the specimens are coated with an approximately 18μm thick coating as broadly explained in the previous work [22].

2.2 AE Equipment

AE activity is recorded using a DiSP system by instrumenting test specimens with two Mistras Group Limited Nano 30 sensors. Sensors were mounted on one side of the specimen by silicone which was simultaneously employed as an acoustic couplant and a mechanical fixture as illustrated in Fig. 3. The correct mounting of the sensors is verified by Hsu-Nielson (H-N) source [22] with a response above 98 dB [23]. The noise threshold is set to 44.9 dB based on the previous researches on steel [19, 24, 25]. AE signal parameters (amplitude, duration, rise time and counts), cycles, and load data are captured throughout the entire fatigue life.

In order to locate the AE source location, an experimentally derived wave speed (5500 m/s) is exploited and the co-ordinates of the sensors (the distance between sensors is 85 mm) are hired as an input to the DiSP system. The integrated

standard algorithm in the AEwin software is employed for calculating the location.

2.3 DIC Equipment

Digital imaging correlation monitoring is prepared before starting the test. A speckle pattern is applied to one side of the specimen (on the opposite face to the AE sensors) using spray paint. The DIC is a non-contact optical technique that provides full-field displacement measurements of a structure. DIC images are collected every 1000 cycles using a Dantec Dynamics (Q-400) system which is triggered from the MTS controller whilst holding the specimen briefly at maximum load. Figure 4(a) explains the load history (red circle refers to the DIC image capturing), Fig. 4(b) schematically shows the test set-up, and Fig. 4(c) displays the arrangement of the test set-up with both DIC and AE systems in place.

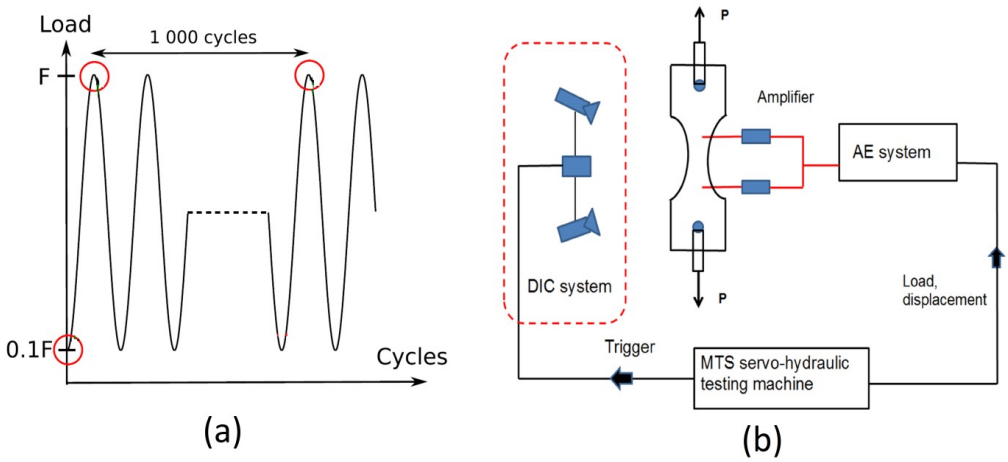

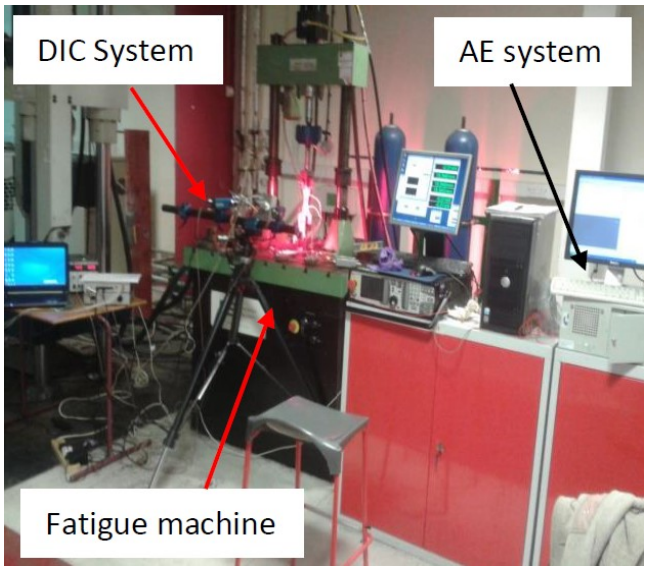

Fig. 4. (a) DIC image captured during the load history (b) schematic diagram of fatigue test (c) the test set up arrangement with both the DIC and AE systems in place.

3. Results and Discussion

3.1 Physical observations

Visual inspection of the tested specimens at the end of the test indicates that the crack propagation starts from the area close to the welding region, due to stress concentration effects, and then propagates parallel through the specimen section until the final failure. The crack cross-section is demonstrated in Fig. 5 with more details of the fracture surface. It is clear that the crack starts propagating horizontally, creating a straight fracture surface (SFS) for an additional 2–3mm away from the one edge. Later, the fracture surface becomes curved then followed by the final failure. This is attributed to the local plane stress field due to the small thickness of the specimen plate. Therefore, the crack starts to propagate horizontally under the application of the tensile stress and final fracture occurs as a result of shear stresses which are at 45° [26]. Moreover, the visual inspection displays that there is flaking in the e-coating layer or DIC paint near the weld because of high-stress concentration in this area.

3.2 AE and DIC results

Crack mouth opening displacement (CMOD) is extracted from the captured DIC data. Two points are selected, one on each side of the crack. The relative movement of these two-pixel subsets on either side of the crack is employed to determine the

CMOD. One value is extracted for every one-thousand cycles. Figure 6 displays the crack mouth opening displacement versus the number of cycles.

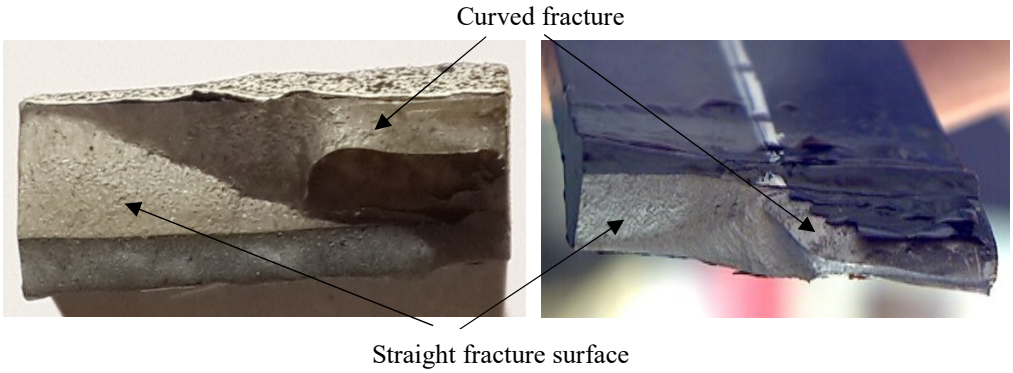

Fig. 5. Crack cross-sections after the final failure.

Since the observed AE behavior is repeatable for all tested specimens, results from only one test under 400 MPa will be presented in this paper. It should be noted that it is the intention of the authors to apply the analysis procedure to signals from located AE events only. Therefore, only AE sources with high energy which hit the two sensors are considered as an event to be used in the analysis. Thereafter, in order to isolate acoustic emission signals (associated with fatigue crack propagation) from other sources (e.g. noise related to surface rubbing at the pins, environmental noise, and the other unknown sources generated outside the test specimens) the recorded data are filtered. It is done based on source location by a narrow region containing the fatigue crack (the area of interest covers 15mm on each side of the weld center) hiring the AE system source location software. Then data from one sensor only considered in the analysis to prevent data repetition.

To validate and support the understanding of the collected AE data, the cumulative AE energy (measured area under rectified AE signal envelope) compared with crack mouth opening displacement as a function of time is illustrated in Fig. 6. It is apparent from the figure that the AE energy signals are distributed throughout the cycle range and in general exhibit a very good correlation with crack propagation rates. As typically expected in metal fatigue, the rate increases exponentially as soon as the crack begins to grow. The crack growth rate increases and then the final failure occurs after 33444 cycles. These results show the ability of using AE monitoring to provide feedback on the structural integrity.

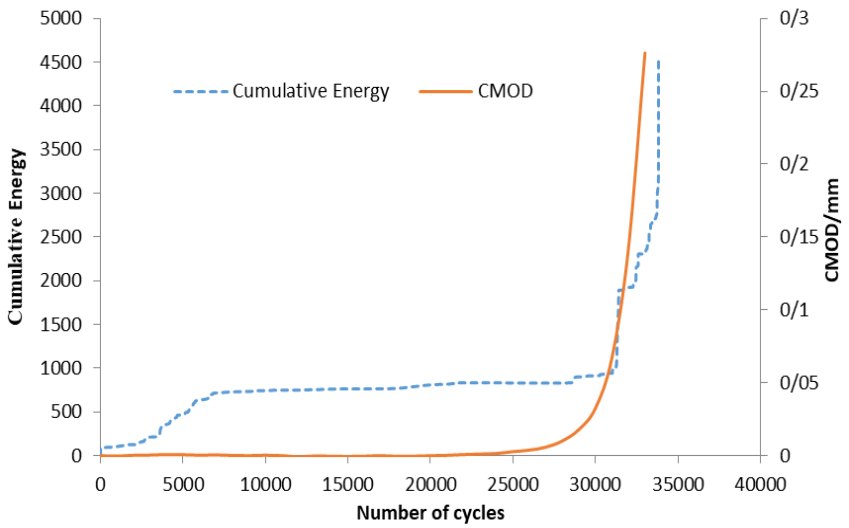

Fig. 6. Trend of event rate for fatigue test and CMOD.

Figure 7 displays the AE activity in terms of signal amplitude together with the CMOD versus the number of cycles. From the figure, three zones have been highlighted as zone 1, zone 2 and zone 3 based on visual inspection of the specimen fracture surface, DIC measurements, and previous investigations. Signals from these zones are believed to be generated by a variety of processes other than crack extension during the test such as corrosion product, micro-cracking, macro-cracking, propagation of cracking, separation of the e-coating layer, and DIC paint from the specimen surface.

Zone 1 refers to the high amplitude signals occurring during the initial stage of the test and it is likely that these signals are because of stretching and loading of the specimen. The next AE activity region (zone 2) could be correspondent to the various damage mechanisms such as flaking in the e-coating layer and flaking in the DIC paint close to the weld area. It is due to high-stress concentrations (weld toe), the difference between elasticity of specimen, e-coating layer, and DIC paint. Examples of the e-coating and DIC paint flaking after the end of the test are shown in Fig. 8.

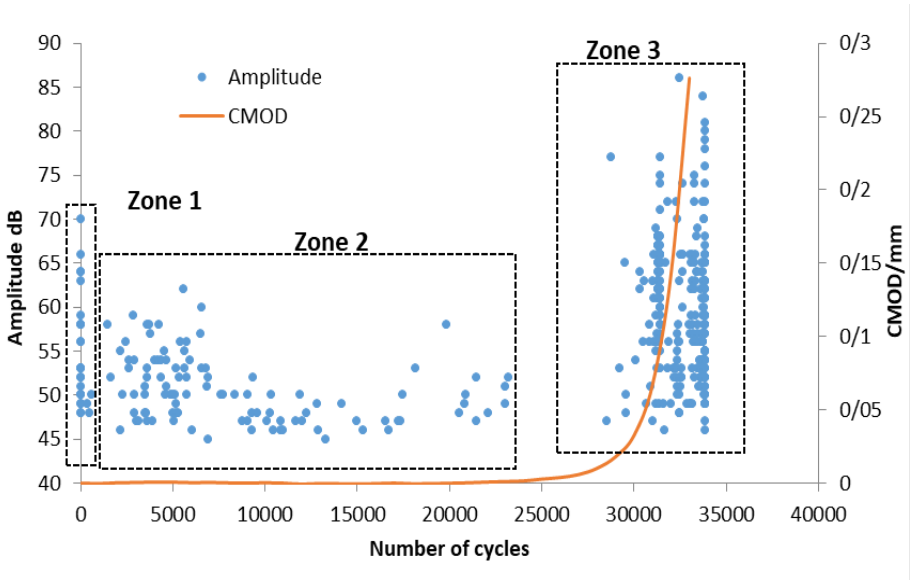

Fig. 7. Amplitude of the detected signals during the investigation.

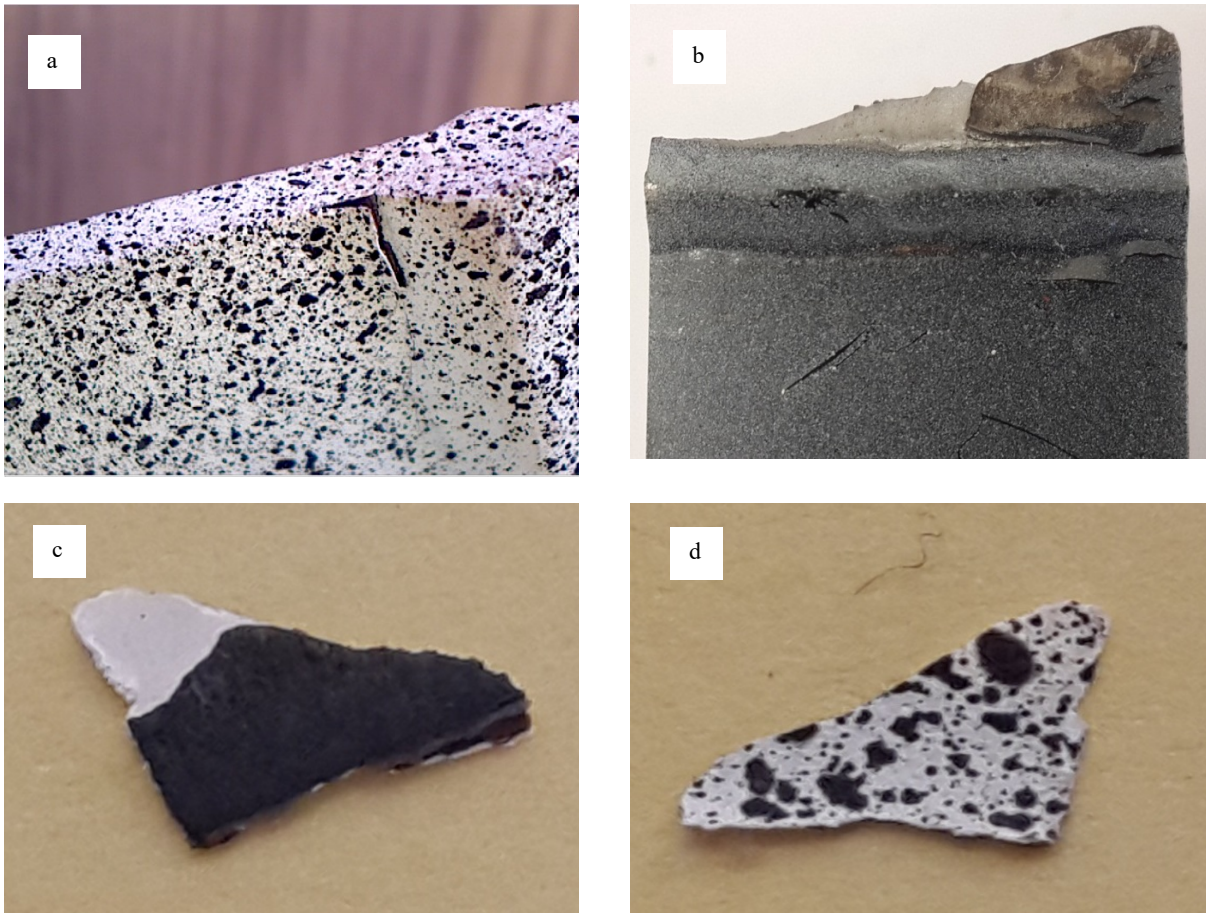

Fig. 8. Specimen after fracture (a) front side (b) rear side which is opposite to DIC cameras (c, d) reveal the flake in the e-coating layer and DIC paint, respectively.

In addition, the DIC visualization presented in Fig. 9 shows the difference in out of plane (z) displacement (axis normal to the specimen surface) between two points. One of which is on the weld metal (WM) and the other one is located on the base metal (BM). As the specimen stretches because of the loading, the delamination occurs in the e-coating at the weld area which increases with loading cycles. This increase then leads to an upward or radially motion outwards the e-coating layer and DIC paint causing a surface crack to form in both of them. This is obvious from visual inspection for both specimen faces (rear and front face) that flaking in the e-coating layer on the rear side which is on opposite the side to DIC cameras and could not detect by the DIC system (Fig. 8b).

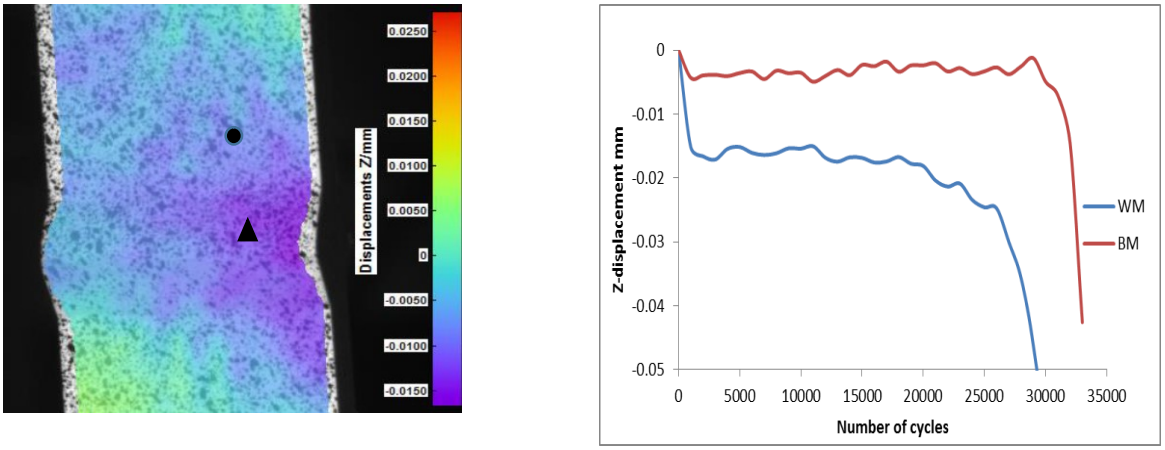

(a) (b)

Fig. 9. (a) Flake in the DIC paint, ● base metal (BM) point and ▲ weld metal (WM) point (b) The DIC Out of plane displacement for base metal and weld surface.

The last high-amplitude group of AE signals (zone 3) corresponds to macro-crack propagation. At this zone, the CMOD reading suddenly increases to its maximum value (Fig. 7).

In order to distinguish between the different fracture modes, the AE signal features are employed. The AE signals are further investigated to gain a deep understanding to explain the transition between different cracking modes that can be examined by RA value which also takes into account the signals' amplitude [6].

Figure 10 a–c plot the AF versus RA values for the different selected zones. Figure 10a shows AF versus RA for zone 1 which is associated with the specimen stretching and could also stem from the plastic deformation. It can be seen that most data points have various AF and low RA values (less than 2 ms/v). Therefore, based on Fig. 2, this indicates that type of crack is associated with tensile damage [9, 11]. For zone 2 (Fig. 10b), the RA value has a wide distribution (RA values up to 15 ms/v and AF values up to 50). This is attributed to delamination in the e-coating layer and DIC paint, possibly due to macro-crack formation which is leading to material volume increase. Thereby, leads to expansion and cracking of the outer layer of e-coating and DIC paint.

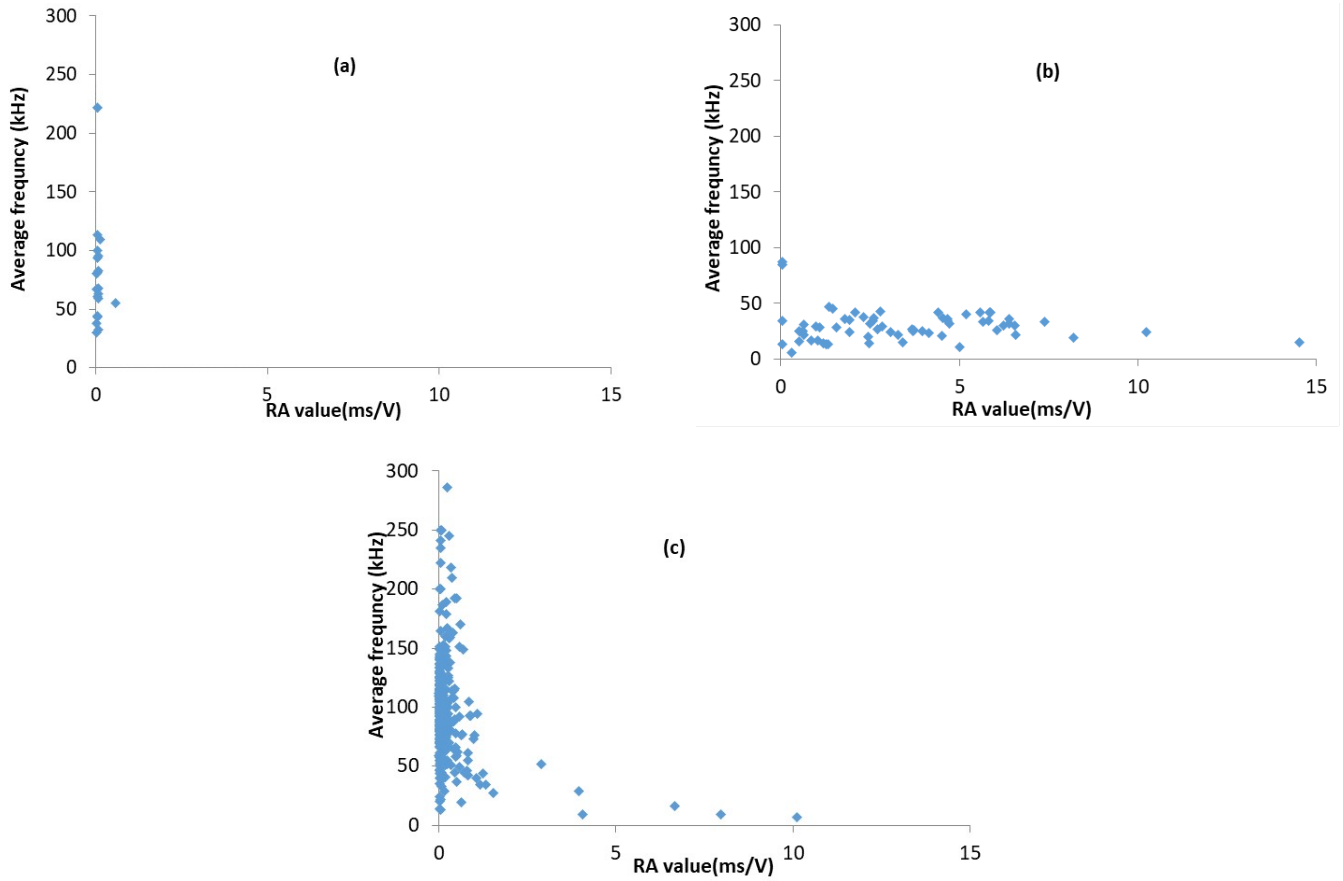

Fig. 10. Relation between RA value and average frequency of (a) zone 1, (b) zone 2, and (c) zone 3.

Figure 10c displays the relationship between RA value and AF associated with the crack region in the last stage of the test in which the transition between different cracking modes occurs from a straight fracture surface to a curved surface shape. Thus, based on Fig. 2, this indicates that the crack type is mixed between two modes, tensile crack and shear mode movement during the final cycles of the test. This issue is consistent with the findings in [9, 11].

Figure 10 demonstrates different mechanisms related to different RA/AF value. Zone 3 is a mixed mode area of both tensile and shear movement whilst zone 1 is purely tensile and zone 2 is almost purely shear. It has been shown that by hiring AE and the relationship between RA and AF value, the crack area can be located and identified. The small specimen size and the sensitivity of the sensors provide accurate capture of these changes as the crack develops [16]. Hence, it could be possible to provide a failure alarm and location to the structure prior to any deformation. Furthermore, by knowing the crack type, it is possible to identify its severity level, then it is possible to identify whether maintenance is needed. This ability is in great demand and is vital to maintain the structure both for safety and economic considerations.

4. Conclusions

The AE analysis is successfully hired to determine crack movements and classify it in accordance with the observations made during fatigue testing. The AE method not only can detect the e-coating layer and DIC paint cracking, also evidence of the fatigue process can be observed. Therefore, this technique is successfully utilized to assess the damage of high-strength steel samples. It is shown that micro-cracks and crack propagation could be detected. The correlation of AE parameters with damage accumulation and the fracture mode has been used to evaluate different crack types. The results have demonstrated that the AE technique is valid for monitoring and hence has the potential for monitoring real structures such as automobile chassis structures. Thus, the findings offer encouragement to the usage of the AE technique to detect the remaining life in fatigue tests and also to enable a warning against final failure.

Acknowledgments

The authors would like to thank Iraqi Ministry of Electricity - General Company of Electrical Energy production - Basrah, Iraqi Ministry of Oil – Gas Filling Company, the Iraqi Ministry of Higher Education and Scientific Research – Basrah University for supporting this research, and the technical staff of Cardiff School of Engineering for their kind assistance with the testing program.

Conflict of Interest

The author(s) declared no potential conflicts of interest with respect to the research, authorship and publication of this article.

Funding

The author(s) received no financial support for the research, authorship and publication of this article.

References

[1] Shrama, K., Clarke, A., Pullin, R., Evans, S.L., Detection of Cracking in Mild Steel Fatigue Specimens Using Acoustic Emission and Digital Image Correlation. *The 31st Conference of the European Working Group on Acoustic Emission (EWGAE),* Dresden, We.4. B.2, 2014.

[2] Al-Jumaili, S. K., Holford, K. M., Eaton, M. J., McCrory, J. P., Pearson, M. R., Pullin, R., Classification of acoustic emission data from buckling test of carbon fibre panel using unsupervised clustering techniques, Structural Health Monitoring, 14(3) (2015) 241-251.

[3] Miller, R. K., McIntire, P., *Acoustic Emission Testing. NDT Handbook*. American Society for Non-destructive Testing, 2005.

[4] Behnia, A., Chai, H. K., Shiotani, T., Advanced structural health monitoring of concrete structures with the aid of acoustic emission. *Construction and Building Materials*, 65 (2014) 282-302.

[5] Carpinteri, A., Lacidogna, G., Accornero, F., Mpalaskas, A.C., Matikas, T.E., Aggelis, D.G., Influence of damage in the acoustic emission parameters. Cement and Concrete Composites, 44 (2013) 9-16.

[6] TC212-ACD, R.I.L.E.M., acoustic emission and related NDE techniques for crack detection and damage evaluation in concrete. Materials and Structures, 43 (2010) 1183-1186.

[7] Ohno, K. and Ohtsu, M., Crack classification in concrete based on acoustic emission. *Construction and Building Materials*, 24(12) (2010) 2339-2346.

[8] Shahidan, S., Pulin, R., Bunnori, N.M., Holford, K.M., Damage classification in reinforced concrete beam by acoustic emission signal analysis. *Construction and Building Materials*, 45 (2013) 78-86.

[9] Elfergani, H.A., Pullin, R. and Holford, K.M., Damage assessment of corrosion in prestressed concrete by acoustic emission. *Construction and Building Materials*, 40 (2013) 925-933.

[10] Kordatos, E. Z., Aggelis, D. G., Matikas, T. E. Monitoring mechanical damage in structural materials using complimentary NDE techniques based on thermography and acoustic emission. *Composites Part B: Engineering*, 43(6) (2012) 2676-2686.

[11] Aggelis, D. G. Classification of cracking mode in concrete by acoustic emission parameters. *Mechanics Research Communications*, 38(3) (2011) 153-157.

[12] McCrory, J., Al-Jumaili, S. K., Pearson, M., Eaton, M., Holford, K., Pullin, R., Automated corrected MAR calculation for characterisation of AE signals. *The 31st Conference of the European Working Group on Acoustic Emission (EWGAE)*, Dresden, Germany, 2014.
[13] Al-Jumaili, S.K., Eaton, M.J., Holford, K.M., McCrory, J., Pullin, R., Damage Characterisation in Composite Materials under Buckling Test Using Acoustic Emission Waveform Clustering Technique. *The 53rd Annual Conference of the British Institute for Non-Destructive Testing*, UK, 2014.
[14] McCrory, J. P., Al-Jumaili, S. K., Crivelli, D., Pearson, M. R., Eaton, M. J., Featherston, C. A., Guagliano, M., Holford, K. M., Pullin, R., Damage classification in carbon fibre composites using acoustic emission: A comparison of three techniques. *Composites Part B: Engineering*, 68 (2015) 424-430.
[15] Crivelli, D., Guagliano, M., Eaton, M., Pearson, M., Al-Jumaili, S., Holford, K., Pullin, R., Localisation and identification of fatigue matrix cracking and delamination in a carbon fibre panel by acoustic emission. *Composites Part B: Engineering*, 74 (2015) 1-12.
[16] Aggelis, D.G., Kordatos, E.Z. and Matikas, T.E., Acoustic emission for fatigue damage characterization in metal plates. *Mechanics Research Communications*, 38(2) (2011) 106-110.
[17] Aggelis, D.G., Verbruggen, S., Tsangouri, E., Tysmans, T., Van Hemelrijck, D., Characterization of mechanical performance of concrete beams with external reinforcement by acoustic emission and digital image correlation. *Construction and Building Materials*, 47 (2013) 1037-1045.
[18] Pullin, R., Eaton, M.J., Hensman, J.J., Holford, K.M., Worden, K. and Evans, S.L., Validation of Acoustic Emission (AE) Crack Detection in Aerospace Grade Steel Using Digital Image Correlation. *Applied Mechanics and Materials*, 24 (2010) 221-226.
[19] Pullin, R., Clarke, A., Eaton, M.J., Holford, K.M., Evans, S.L., McCory, J.P., Detection of cracking in gear teeth using Acoustic Emission. *Applied Mechanics and Materials*, 24-25 (2010) 45-50.
[20] Kovac, J., Alaux, C., Marrow, T.J., Govekar, E., Legat, A., Correlations of electrochemical noise, acoustic emission and complementary monitoring techniques during intergranular stress-corrosion cracking of austenitic stainless steel. *Corrosion Science*, 52(6) (2010) 2015-2025.
[21] SAEJ2332 Cosmetic corrosion Lab test SAE J2332. The Engineering Society for Advance Mobility Land Sea and Space 1998-06 2002.
[22] Hsu, N. N., Breckenridge, F. R., Characterization and Calibration of Acoustic Emission Sensors. *Materials Evaluation*, 39(1) (1981) 60-68.
[23] ASTME976 Standard guide for determining the reproducibility of acoustic emission sensor response. American Society for Testing and Materials 2001.
[24] Baxter, M., Damage Assessment by Acoustic Emission (AE) During Landing Gear Fatigue Testing, Ph.D. Thesis, School of Engineering, University of Wales Cardiff, Cardiff, UK, 2007.
[25] Al-Jumaili, S.K., Pearson, M.R., Holford, K.M., Eaton, M.J. and Pullin, R., Acoustic emission source location in complex structures using full automatic delta T mapping technique. *Mechanical Systems and Signal Processing*, 72 (2016) 513-524.
[26] Hearn, E.J., Mechanics of materials 1: an introduction to the mechanics of elastic and plastic deformation of solids and structural components. Butterworth-Heinemann, 1997.